International Journal of Chemical, Materials and Biomolecular Sciences
ISSN: 2415-6620
Vol:8, No:7, 2014

Mercury Removing Capacity of Multiwall Carbon Nanotubes as Detected by Cold Vapor Atomic Absorption Spectroscopy: Kinetic & Equilibrium Studies

Yasser M. Moustafa, Rania E. Morsi, Mohammed Fathy

***Abstract*—**Multiwall carbon nanotubes, prepared by chemical vapor deposition, have an average diameter of 60-100 nm as shown by High Resolution Transmittance Electron Microscope, HR-TEM. The Multiwall carbon nanotubes (MWCNTs) were further characterized using X-ray Diffraction and Raman Spectroscopy. Mercury uptake capacity of MWCNTs was studied using batch adsorption method at different concentration ranges up to 150 ppm. Mercury concentration (before and after the treatment) was measured using cold vapor atomic absorption spectroscopy. The effect of time, concentration, pH and adsorbent dose were studied. MWCNT were found to perform complete absorption in the sub-ppm concentrations (parts per billion levels) while for high concentrations, the adsorption efficiency was 92% at the optimum conditions; 0.1 g of the adsorbent at 150 ppm mercury (II) solution. The adsorption of mercury on MWCNTs was found to follow the Freundlich adsorption isotherm and the pseudo-second order kinetic model.

***Keywords*—**Cold Vapor Atomic Absorption Spectroscopy, Hydride System, Mercury Removing, Multi Wall Carbon Nanotubes.

I. Introduction

THE available source of clean water, the shrinking levels of surface water and waste waters pollution, and contamination of environment by toxic pollutants have emerged as the most serious problems facing our globe in the twenty-first century. Removal of inorganic and organic pollutants from waters is considered as one of the major investigations in the last few decades.

Mercury is well known to be one of the most toxic metals known in natural ecosystems. During the 20th century there were several major Hg poisoning catastrophes as Hg is deemed cumulative and persistent in human body and the environment as well [1]. Long-term exposure to very low levels of mercury even in water is dangerous for humans [2], [3]. It is known that Hg may be absorbed through the gastro-intestinal tract and through the skin and lungs [4]. Soluble compounds of mercury are particularly toxic because their adsorption is rapid. Nevertheless, Hg is still being used worldwide in applications such as barometers, thermometers, pumps, and lamps to name a few. Industries mainly responsible for the dispersion of mercury are: the chloro-alkali, paint, oil refining, and rubber processing and fertilizer industries [5].

An improved understanding of the toxic health effects of mercury and its bio-accumulative properties has led to greater regulatory control. The EPA has initiated regulations to control mercury emissions to air through the Clean Air Act (CAA); water through the Clean Water Act (CWA) Safe Drinking Water Act (SDWA); and from wastes and products through Resources Conservation and Recovery Act (RCRA) [6], [7]. The EPA has established a maximum contamination level (MCL) for mercury to be 2 µg/L in drinking water. The World Health Organization (WHO) also recommends a maximum uptake of 0.3 mg per week and 1 µg/L as the maximum acceptable concentration in drinking water [8]. Thus, accurate and precise qualitative and quantitative detection of mercury in aqueous media is highly recommended.

The direct determination of trace concentrations of heavy metal ions has many problems. Such problems are associated with matrix interferences and low sensitivity, especially in extremely low concentrations. The direct determination by atomic spectroscopy can be problematic. For example, the determination of mercury by flame atomic absorption spectrometry is limited to high concentrations of mercury owing to the poor detection limit offered by the technique 200 µg /L. While the use of electro thermal atomic absorption spectrometry (ETAAS), although it allows better detection limits (2 µg /L, suffers from matrix interference as the high volatility of mercury restricts the ashing temperature.

One of the most common analytical approaches for the determination of total mercury at lower concentrations is cold vapor atomic absorption spectrometry (CVAAS) with its high sensitivity and selectivity as well as extremely low detection limit (1 µg/L) [9]–[12].

A number of approaches have been suggested for the removal of mercury from aqueous solutions. The techniques include reduction, precipitation, ion exchange, reverse osmosis, adsorption, coagulation, etc. Though bulk techniques like simple filtration or precipitation are suitable for removing a significant fraction of the metal, they are unable to decrease the concentration of contaminant from percentage to ppm level and/or even in ppb level [13]. Thus, there is an urgent

Yasser M. Moustafa is with the Analysis and Evaluation Department, Egyptian Petroleum Research Institute, EPRI, Cairo, Egypt (corresponding author e-mail: Corresponding author: ymoustafa12@yahoo.com).

Rania E. Morsi and Mohammed Fathy are with the Analysis and Evaluation Department, Egyptian Petroleum Research Institute, EPRI, Cairo, Egypt.

need for an adequate step which can address metal removal in ppb level to meet the environmental agency regulations.

In recent years, considerable attention has been given to remove mercury by adsorption process on various adsorbents [13]–[20]. Nanomaterials were heavily researched for its utilization in water treatment [21], [22]. Due to their nanosize, large surface area, high mechanical strength and remarkable electrical conductivities, carbon nanotubes (CNTs) are considered as superior candidates for a wide range of promising applications [23], [24]. For example, the suitability of CNTs in removing different types of water contaminants was investigated by many researchers in the last few years [25]. Their hollow and layered nano-sized structures make them a promising adsorbent material that can substitute different materials in many ways [26].

The adsorption of heavy metals by nanotubes has been studied for different elements such as lead [27], [28], fluoride [29], cadmium [30], Zinc [31], Uranium [32], Cobalt [33], Europium [34] and Nickel [35]. Shadbad et al. [36] studied the efficiency of mercury (II) removal by multi-walled carbon nanotubes at relatively high conc. (50 ppm) measured by the low detection limit of FAAS.

In this work, a detailed study was performed, covering concentrations from 10 ppb to 150 ppm including the equilibrium and kinetics of batch adsorption for mercury (II) removal from aqueous solutions by MWCNTs. Mercury concentration (before and after the treatment) was measured using cold vapor atomic absorption spectroscopy. The technique provides a fast and sensitive detection with low detection limit to measure traces after the treatment with detection limit of, as low as 1 μg/L.

II. Materials and Methods

A. Material

Multiwall - carbon nanotubes were prepared by chemical vapor deposition (CVD) method and were kindly supplied from EPRI Nano-Technology Center.

B. Mercury Uptake

1. Batch Method

Assessment of Hg (II) adsorption by MWCNTs is carried out by batch adsorption experiments. Batch mode sorption experiments were performed in sealed glass flasks at room temperature. Pre-weighted amounts of the MWCNTs were added to glass flasks containing 20 ml of the desired concentration of aqueous mercury solution. The glass flasks were stirred for the designated time, filtered and then subjected to Hg concentration measurement. The effects of the dosage of MWCNTs (0.01, 0.05 and 0.1 g), contact time (10–120 min) and the initial Hg concentration (10 ppb to 150 ppm) in addition to the pH range, from 1 to 9, were investigated. The amount of Hg adsorbed on the MWCNTs was determined by the difference of the initial concentration (Ci) and the equilibrium concentration (Ce).

The percentage removed of Hg ions from the solution was calculated as following:

$$\%removal = (C_i - C_e)x100/C_i \quad (1)$$

The adsorption capacity (qe) was calculated as following:

$$q_e(mg/g) = (C_i - C_e)xV/M \quad (2)$$

where, V = volume of the Hg^{2+} solution (L), M = weight of adsorbent (g).

2. Determination of Hg Concentration "Hydride System Attached to Cold Vapor Atomic Absorption Spectrometer"

Hg concentration was measured using hydride system connected to cold vapor atomic absorption spectrometry (CV-AAS). In this technique, the sample solution as well as acid and reductant are aspirated using a multi-channel peristaltic pump. Acidified sample and reductant get into contact in the reactor for sample reduction where the atomic Hg vapor as well as hydrogen gas liberated in this process. The gaseous reaction products are carried by the argon stream to the gas-liquid separator. There, the gas phase (Hg vapor, argon and hydrogen) and the liquid phase are separated where the residual liquid is pumped off. Gas path selector leads the separated gases to a gold collector for Hg enrichment. The enriched Hg will then be liberated in baking out the gold collector and carried out to the quartz cell by an argon stream where the free Hg atoms absorb the primary radiation at the specific resonance line.

III. Results and Discussion

A. Characterization of Carbon Nanotubes

The MWCNTs were observed by high-resolution transmission electron microscope (HRTEM), as shown in Fig. 1. The morphology of MWCNTs was tubular-like well-defined multiwall structure. The average diameter for different samples was about 60 to100 nm.

Fig. 2 shows the X-ray diffraction of multiwall carbon nanotubes. The diffraction patterns of multiwall carbon nanotubes consisted of many crystalline peaks and the prominent peak at about $2\theta = 26^{o}$ can be attributed to the (0 0 2) reflection of carbon [37], [38].

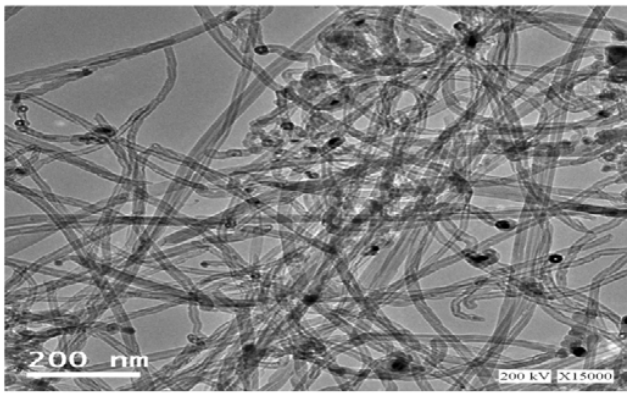

Fig. 1 HR-TEM image of MWCNTs

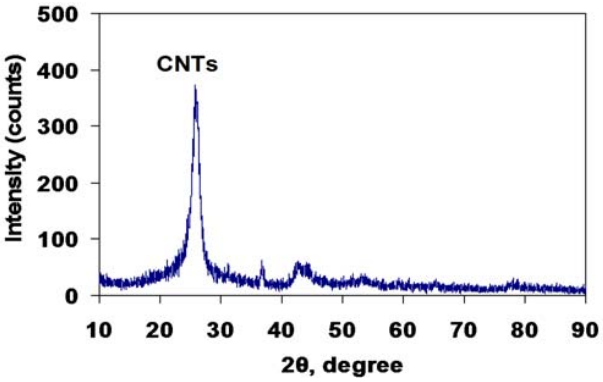

Fig. 2 X-ray diffraction (XRD) pattern of MWCNTs

Fig. 3 shows the Raman spectrum of MWCNTs. The two main typical graphite bands are present in the Raman spectrum of MWCNTs; the band at 1586.89 cm^{-1} (G band) is assigned to the in-plane vibration of the C–C bond (G band) typical of defective graphite-like materials and the band at 1311.74 cm^{-1} (D band) is activated by the presence of disorder in carbon systems [39].

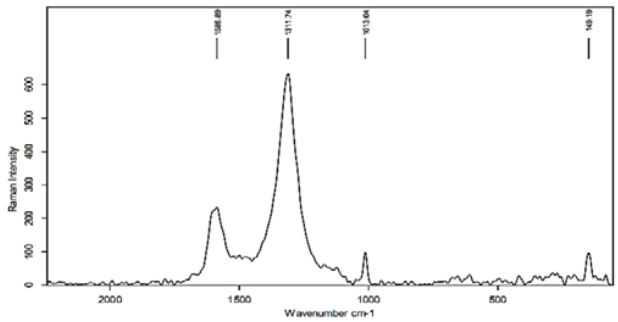

Fig. 3 Raman spectrum of MWCNTs

B. Mercury Uptake

1. Effect of Adsorbent Dose

Different adsorbent doses were used to investigate the efficient amount of adsorbent required to remove a specific concentration of mercury at certain conditions. Three different weights of MWCNTs were used; 0.01, 0.05 and 0.1g. In addition, the experiments were carried out at different time intervals (10-120 min), as shown in Fig. 4, to identify the kinetic of adsorption mechanism. The adsorption efficiency % of Hg is generally enhanced when the amount of MWCNTs is increased which can be attributed to the increased availability of adsorption sites. The same behavior was found in all tested time intervals range. The sorption mechanism was mainly attributed to the interactions between the metal ions and the different binding sites; the surface functional groups, the multilayers and the hollow area inside the tubes. The comparison of CNTs with other adsorbents suggests that CNTs have great potential applications in environmental protection particularly in trace metals removal from water [14]–[20].

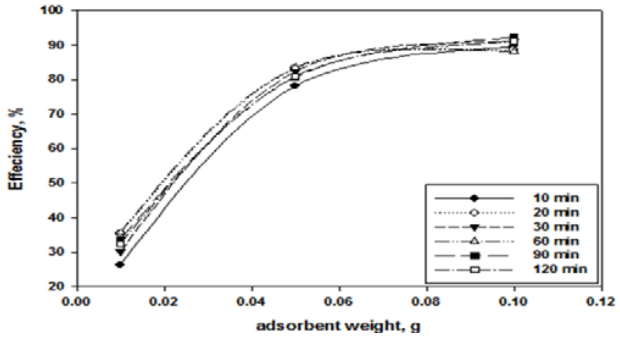

Fig. 4 Effect of adsorbent weight on Hg uptake efficiency at different time intervals using initial Hg concentration of 100 ppm

2. Effect of pH

The pH value plays an important role with respect to the adsorption of particular ions on functionalized CNTs due to its effect on the surface charge. Fig. 5 shows the removal of Hg ions by MWCNT at different values of pH. The low Hg^{2+} adsorption that took place at low pH can be attributed in part to competition between H^+ and Hg^{2+} ions on the same sites as at pH<8, the predominant Hg species is Hg^{2+} ions [40]. As the surface of CNTs becomes more negative with the increasing of pH, the electrostatic attraction increases and thus results in adsorption of more Hg^{2+} onto MWCNTs. In the pH range of 5-8, the removal of Hg increased and reached a maximum. At pH 9, a slight decrease of removal of mercury due to the increase in the hydroxide ion concentration leading to the formation of Hg negative hydroxide species and consequently, decrease in Hg uptake on the surface of functionalized negatively charged MWCNTs.

At relatively higher concentration of Hg ions, 10 ppm, the effect of pH was found to be less pronounced and reached maximum at lower pH value due to the presence of much more Hg ions which allow higher competition against the H^+ ion in the low pH range. At higher pH, a slight decrease in the uptake efficiency was also due to the formation of negative Hg species as mentioned before.

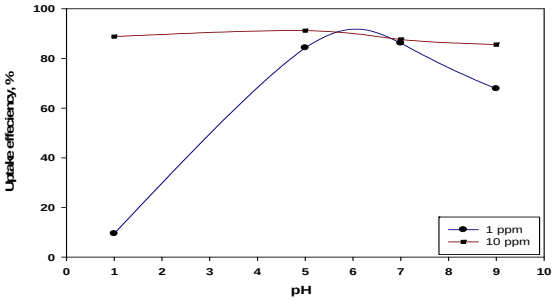

Fig. 5 Effect of pH on Hg uptake efficiency

3. Effect of Contact Time & the Kinetic Studies

An ideal adsorbent for wastewater pollution control must have not only a large adsorption capacity but also a fast rate of adsorption. These requirements are more urgent in such case as in mercury due to its low vapor pressure. Fig. 6 shows the effect of contact time on the mercury uptake efficiency using

different doses of the adsorbent. As shown in the figure the adsorption efficiency was very fast and reached the equilibrium state within 20 min. after which it reached a constant value. At this point, the amount of metal ions being adsorbed on the material is in a state of dynamic equilibrium with the amount of metal ions desorbed from the adsorbent. Equilibrium time achieved within 20 min. Obviously, the adsorption rates were very fast; comparing with some other mercury adsorbents [41]–[43]. This relatively fast rate of adsorption is advantageous in the mercury removal process.

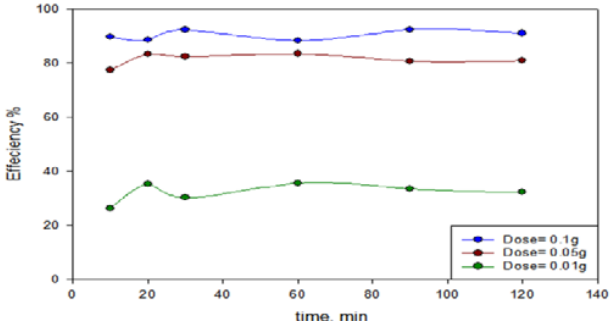

Fig. 6 Effect of contact time on Hg uptake efficiency using different adsorbent doses at initial mercury concentration of 100 ppm

For further analysis of the results, several kinetic models are used to describe the adsorption kinetics. Four common equations were tested to find the best-fitted model for the obtained experimental data. The corresponding linear equations are given below.

The pseudo-first order kinetic model was suggested by Lagergren [44] for the adsorption of solid/liquid systems and its linear form can be formulated as:

$$Ln\ (q_e - q_t) = (Ln(q_e) - K_{1p}t)/2.303 \quad (3)$$

The 1st order kinetic model linear form can be formulated as:

$$Log\ ((q_e - q_t)/\ q_e) = K_1 t/2.303 \quad (4)$$

Ho and McKay's pseudo-second order kinetic model [45] can be expressed as:

$$t/q_t = 1/2kq_e^{\ 2} + t/q_t \quad (5)$$

The 2nd order kinetic model linear form can be formulated as:

$$1/(q_e - q_t) = 1/q_e + K_{p2}t \quad (6)$$

where q_e and q_t are the amount of Hg (II) adsorbed at equilibrium (mg.g^{-1}) and at time t, respectively. k_1 is the equilibrium rate constant of the pseudo-first order adsorption (min^{-1}). k_{1p} is the equilibrium rate constant of the first order adsorption (min^{-1}). k_2 is the equilibrium rate constant of the pseudo-second order adsorption (g mg^{-1} min^{-1}) and k_{2p} is the equilibrium rate constant of the second order adsorption (g^{-1} mg^{-1} min^{-1}).

The experimental data have been fitted by the above-mentioned kinetics models and the obtained parameters were listed in the Table I. Based on the analysis of the R^2 of the linear form for the various kinetics models, the pseudo-second order model was more appropriate to describe the adsorption kinetics behaviors for Hg (II) ions onto MWCNTs. Accordingly, the chemisorptions were the rate controlling mechanism. The fitting of the experimental data to the pseudo-second order model for all the adsorbent doses confirm the suggested adsorption mode. They were fully consistent with those drawn from adsorption isotherm analysis as will be discussed later. The fitting results of the pseudo-second order model was shown in the Fig. 7.

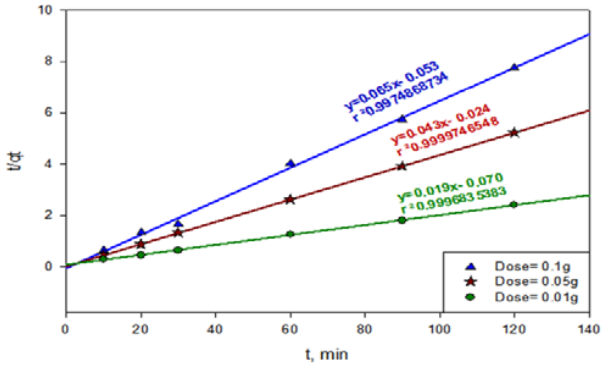

Fig. 7 Adsorption kinetics pseudo-second order model of Hg (II) on MWCTs

TABLE I
KINETICS PARAMETERS FOR HG (II) ADSORPTION ONTO MWCNTS

Dose ,g	Pseudo 1st order		1st order		Pseudo 2nd order			2nd order	
	R^2	K_{p1}	R^2	K_1	R^2	q_e	K_{p2}	R^2	K_2
0.10	0.61	0.04	0.49	-3.80	0.99	15.4	-0.09	0.77	-0.23
0.05	0.51	-0.03	0.85	-1.51	1.000	23.2	0.08	0.93	0.01
0.01	0.85	0.04	0.61	-3.30	1.000	51.6	0.01	0.81	0.05

4. Effect of Initial Concentration & the Adsorption Isotherms

Mercury removal process is required to be effective at very low concentrations. From Fig. 8, the Hg uptake of MWCNTs increases linearly with the increase of the initial concentrations of Hg. Complete removing of mercury ions in the lower range of concentration is achieved as shown in the insert of Fig. 7. At low initial concentrations of Hg (II) ions, the adsorption sites on the adsorbents were sufficient and the Hg (II) uptakes relied on the amount of Hg (II) ions transported from the bulk solution to the surfaces of the adsorbents. However, at higher initial concentrations of Hg (II) ions, the adsorption sites on the surfaces of the adsorbents reach the saturation and the adsorption of Hg (II) ions achieves equilibrium giving incomplete Hg adsorption [46].

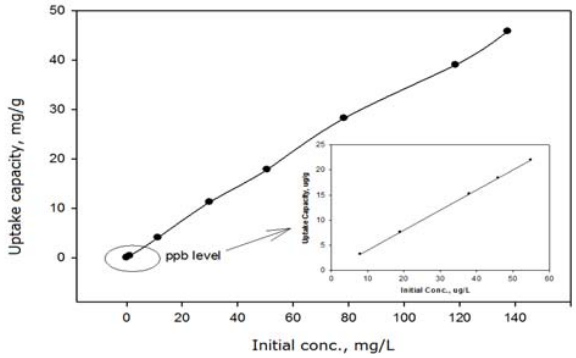

Fig. 8 Effect of initial concentration on the Hg uptake capacity of MWCNTs, the inserted figure shows the complete adsorption of Hg in the sub- and/or the near ppm level, using 0.05 g adsorbent at 20 min

The equilibrium isotherm is fundamental to describe the interactive behavior between the solutes and adsorbents and illuminates the properties and affinity of the adsorbent. Adsorption isotherms describe how adsorbate molecules interact with adsorbent particles. The distribution of Hg (II) ions between the liquid phase and the adsorbent is a measurement of the position of equilibrium in the adsorption process. An accurate mathematical description of equilibrium adsorption capacity is indispensable for reliable prediction of adsorption parameters and quantitative comparison of adsorption behavior for different adsorbent systems or for varied experimental conditions.

In the present study, the adsorption equilibrium data have been analyzed by various isotherm models; Langmuir, Freundlich, Temkin, and Dubinin–Radushkevich (D–R) isotherm, to further investigate the adsorption mechanism.

Langmuir model is based on the assumption that adsorption sites are identical and energetically equivalent, only monolayer adsorption occurs in the process [47]. It can be represented as follows:

$$C_e / q_e = 1/(q_{\max} b) + C_e / q_{\max} \quad (7)$$

where q_e is the amount of Hg (II) ions adsorbed at equilibrium (mg g^{-1}), C is the liquid-phase Hg (II) concentration at equilibrium (mg dm^{-3}), q_{max} is the maximum adsorption capacity of the adsorbent (mg g^{-1}), and b is the Langmuir adsorption constant (dm^3 mg^{-1}), respectively.

Freundlich isotherm model is based on the assumption of an exponentially decaying adsorption site energy distribution [48].

It is applied to describe heterogeneous system characterized by a heterogeneity factor of n. The Freundlich model is expressed as follows:

$$Log\ (q_e) = (1/n)\ Log\ (C_e) + Log\ (K_F) \quad (8)$$

where K_f is the Freundlich isotherm constant, and n (dimensionless) is the heterogeneity factor.

TABLE II
THE ISOTHERMS PARAMETERS OF HG (II) ADSORPTION ONTO MWCNTS

$q_{max,exp}$	Langmuir model			Freundlich			Temkin			D-R model		
	$q_{max,theo}$	b x 10^3	R^2	K_f	n	R^2	A_T	B_T	R^2	K	q_D	R^2
22	71.43	66.79	0.85	-0.37	1.02	0.98	1.11	12.79	0.95	2e-7	10.7	0.84

Temkin isotherm is based on the assumption that the surface of the adsorbents is heterogeneous and the energy of the active sites distributes linearly. It is frequently employed for analysis on chemical adsorptions. The Temkin isotherm can be expressed in its linear form as [49].

$$q_e = B_T Log\ (K_T) + B_T Log(C_e) \quad (9)$$

where B_T is Temkin constant related to the heat of adsorption (KJ/mol) and K_T is empirical Temkin constant related to the equilibrium binding constant related to the maximum binding energy (L.mg^{-1}), (L.mol^{-1})

The D–R isotherm model is usually employed for the determination of the nature of bio-sorption processes as physical or chemical process [50].

$$Ln\ (q_e) = Ln\ (q_D) - K \epsilon^2 \quad (10)$$

where K is the constant related to the mean free energy of sorption, q_D is the theoretical saturation capacity, ϵ Polanyi potential (J. mol^{-1}), which can be calculated as:

$$\epsilon = RT\ Ln\ (1 + (1/C_e)) \quad (11)$$

where R is the gas constant (J $mol^{-1}K^{-1}$), T the absolute temperature (K) and C_e the equilibrium concentration of the adsorbate in aqueous solution (g.L^{-1}).

The experimental adsorption data was fitted based on the mentioned isotherm models. The parameters obtained were all listed in Table II. Based on these results, the correlation coefficients (R^2) of the linear form of Freundlich model were much closer to 1.0 than those of the other models, the coefficients for Temkin and D-R models were higher than 0.9, whereas those for Langmuir model were much lower. From Fig. 9, it was found that the Freundlich theoretically simulated curves as thin solid lines, fitted the experimental data, represented as small dots, in a fairly good way. They all revealed that the Freundlich model provides the most satisfactory description for the Hg (II) adsorption. These finding are well matched with the geometrical structure of the MWCNTs where this adsorbent contains different binding sites; the carboxylic functional groups on the outer surface, the inner hollow area inside the tubes in addition to the inter- and intra-layers sites.

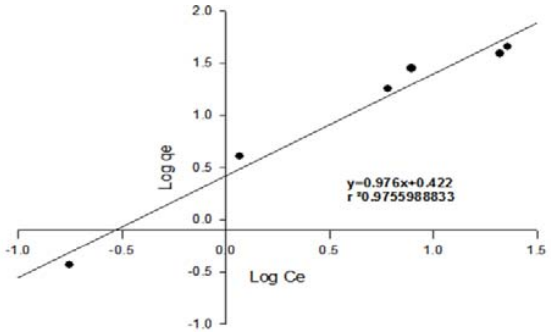

Fig. 9 Freundlich adsorption isotherm of Hg (II) on MWCTs

ACKNOWLEDGMENT

The authors express their Acknowledgment for EPRI-Central analytical Laboratory and EPRI- nano-Technology Center.

REFERENCES

[1] S. Bernard, a Enayati, L. Redwood, H. Roger, and T. Binstock, "Autism: a novel form of mercury poisoning.," *Med. Hypotheses*, vol. 56, no. 4, pp. 462–71, Apr. 2001.

[2] "U.S. EPA, Mercury Study Report to Congress, EPA 452, Executive Summary, EPA OAQPS/ORD, 1997, pp. R97–R105."

[3] W. F. Fitzgerald, D. R. Engstrom, R. P. Mason, and E. A. Nater, "The case for atmospheric mercury contamination in remote areas," *Environ. Sci. Technol.*, vol. 32, no. 1, pp. 1–7, 1998.

[4] P. L. Bidstrup, "Toxicity of Mercury and its Compounds." *Toxic. Mercur. its Compd.*, 1964.

[5] K. Kadirvelu, M. Kavipriya, C. Karthika, N. Vennilamani, and S. Pattabhi, "Mercury (II) adsorption by activated carbon made from sago waste," *Carbon*, vol. 42, no. 4, pp. 745–752, 2004.

[6] "U.S. Environmental Protection Agency (EPA) and Environment Canada. 1999. Update: Binational Toxics Strategy – Mercury Sources and Regulations."

[7] "U.S. EPA. 2005. Great Lakes Pollution Prevention and Toxics Strategy. Background Information on Mercury Sources and Regulations."

[8] C. F. Forster and D. A. Wase, "Biosorbents for metal ions," 1997.

[9] J. C. a. de Wuilloud, R. G. Wuilloud, R. a. Olsina, and L. D. Martinez, "Separation and pre-concentration of inorganic and organo-mercury species in water samples using a selective reagent and an anion exchange resin and determination by flow injection-cold vapor atomic absorption spectrometry," *J. Anal. At. Spectrom.*, vol. 17, no. 4, pp. 389–394, Apr. 2002.

[10] J. L. Capelo, C. D. Dos Reis, C. Maduro, and a Mota, "Tandem focused ultrasound (TFU) combined with fast furnace analysis as an improved methodology for total mercury determination in human urine by electrothermal-atomic absorption spectrometry" *Talanta*, vol. 64, no. 1, pp. 217–23, Sep. 2004.

[11] D. P. Torres, M. A. Vieira, A. S. Ribeiro, and A. J. Curtius, "Determination of inorganic and total mercury in biological samples treated with tetramethylammonium hydroxide by cold vapor atomic absorption spectrometry using different temperatures in the quartz cell," *J. Anal. At. Spectrom.*, vol. 20, no. 4, pp. 289–294, 2005.

[12] B. Welz, "Atomic Absorption Spectrometry (2nd edn.) VCH," New York, p. 279, 1985.

[13] L. Malachowski, J. L. Stair, and J. A. Holcombe, "Immobilized peptides/amino acids on solid supports for metal remediation," *Pure Appl. Chem.*, vol. 76, no. 4, pp. 777–787, 2004.

[14] S. Dutta, A. Bhattacharyya, P. De, P. Ray, and S. Basu, "Removal of mercury from its aqueous solution using charcoal-immobilized papain (CIP).,"*J. Hazard. Mater.*, vol. 172, no. 2–3. pp. 888–96, 30-Dec-2009.

[15] I. Ghodbane and O. Hamdaoui, "Removal of mercury (II) from aqueous media using eucalyptus bark: kinetic and equilibrium studies," *J. Hazard. Mater.*, vol. 160, no. 2, pp. 301–309, 2008.

[16] K. Anoop Krishnan and T. S. Anirudhan, "Removal of mercury(II) from aqueous solutions and chlor-alkali industry effluent by steam activated and sulphurised activated carbons prepared from bagasse pith: kinetics and equilibrium studies.," *J. Hazard. Mater.*, vol. 92, no. 2, pp. 161–83, May 2002.

[17] M. B. Lohani, A. Singh, D. C. Rupainwar, and D. N. Dhar, "Studies on efficiency of guava (Psidiumguajava) bark as bioadsorbent for removal of Hg (II) from aqueous solutions.," *J. Hazard. Mater.*, vol. 159, no. 2–3, pp. 626–9, Nov. 2008.

[18] F. Di Natale, a Lancia, a Molino, M. Di Natale, D. Karatza, and D. Musmarra, "Capture of mercury ions by natural and industrial materials.," *J. Hazard. Mater.*, vol. 132, no. 2–3, pp. 220–5, May 2006.

[19] S. W. Al Rmalli, A. a Dahmani, M. M. Abuein, and A. a Gleza, "Biosorption of mercury from aqueous solutions by powdered leaves of castor tree (Ricinuscommunis L.)," *J. Hazard. Mater.*, vol. 152, no. 3, pp. 955–9, Apr. 2008.

[20] M. Velicu, H. Fu, R. P. S. Suri, and K. Woods, "Use of adsorption process to remove organic mercury thimerosal from industrial process wastewater." *J. Hazard. Mater.*,vol. 148, no. 3. pp. 599–605, 30-Sep-2007.

[21] T. Masciangioli and W. Zhang, "Environmental nanotechnology: Potential and pitfalls," *Environ. Sci. Technol*, vol. 37, p. 102A–108A, 2003.

[22] N. Savage and M. S. Diallo, "Nanomaterials and water purification: opportunities and challenges," *J. Nanoparticle Res.*, vol. 7, no. 4–5, pp. 331–342, 2005.

[23] R. Saito, M. Fujita, G. Dresselhaus, and u M. S. Dresselhaus, "Electronic structure of chiral graphene tubules," *Appl. Phys. Lett.*, vol. 60, no. 18, pp. 2204–2206, 1992.

[24] C. Dekker, "Carbon nanotubes as molecular quantum wires," *Phys. Today*, vol. 52, pp. 22–30, 1999.

[25] M. Meyyappan and D. Srivastava, "Carbon Nanotube: A Big Revolution in a Technology that Thinks Very, Very, Very Small," *IEEE Potentials*, vol. 19, no. 3, pp. 16–18, 2000.

[26] C. P. Nanseu-Njiki, S. R. Tchamango, P. C. Ngom, A. Darchen, and E. Ngameni, "Mercury (II) removal from water by electrocoagulation using aluminium and iron electrodes," *J. Hazard. Mater.*, vol. 168, no. 2, pp. 1430–1436, 2009.

[27] Y.-H. Li, S. Wang, J. Wei, X. Zhang, C. Xu, Z. Luan, D. Wu, and B. Wei, "Lead adsorption on carbon nanotubes," *Chem. Phys. Lett.*, vol. 357, no. 3–4, pp. 263–266, May 2002.

[28] J. Li, S. Chen, G. Sheng, J. Hu, X. Tan, and X. Wang, "Effect of surfactants on Pb(II) adsorption from aqueous solutions using oxidized multiwall carbon nanotubes," *Chem. Eng. J.*, vol. 166, no. 2, pp. 551–558, Jan. 2011.

[29] Y.-H. Li, S. Wang, X. Zhang, J. Wei, C. Xu, Z. Luan, and D. Wu, "Adsorption of fluoride from water by aligned carbon nanotubes," *Mater. Res. Bull.*, vol. 38, no. 3, pp. 469–476, 2003.

[30] Y.-H. Li, S. Wang, Z. Luan, J. Ding, C. Xu, and D. Wu, "Adsorption of cadmium (II) from aqueous solution by surface oxidized carbon nanotubes," *Carbon N. Y.*, vol. 41, no. 5, pp. 1057–1062, 2003.

[31] C. Lu and H. Chiu, "Adsorption of zinc(II) from water with purified carbon nanotubes," *Chem. Eng. Sci.*, vol. 61, no. 4, pp. 1138–1145, Feb. 2006.

[32] D. Shao, Z. Jiang, X. Wang, J. Li, and Y. Meng, "Plasma induced grafting carboxymethyl cellulose on multiwalled carbon nanotubes for the removal of UO_2^{2+} from aqueous solution," *J. Phys. Chem. B*, vol. 113, no. 4, pp. 860–864, 2009.

[33] H. Chen, J. Li, D. Shao, X. Ren, and X. Wang, "Poly (acrylic acid) grafted multiwall carbon nanotubes by plasma techniques for Co (II) removal from aqueous solution," *Chem. Eng. J.*, vol. 210, pp. 475–481, 2012.

[34] C. L. Chen, X. K. Wang, and M. Nagatsu, "Europium Adsorption on Multiwall Carbon Nanotube/Iron Oxide Magnetic Composite in the Presence of Polyacrylic Acid," *Environ. Sci. Technol.*, vol. 43, no. 7, pp. 2362–2367, Feb. 2009.

[35] M. I. Kandah and J.-L. Meunier, "Removal of nickel ions from water by multi-walled carbon nanotubes.," *J. Hazard. Mater.*, vol. 146, no. 1–2, pp. 283–8, Jul. 2007.

[36] M. J. Shadbad, A. Mohebbi, and A. Soltani, "Mercury(II) removal from aqueous solutions by adsorption on multi-walled carbon nanotubes," *Korean J. Chem. Eng.*, vol. 28, no. 4, pp. 1029–1034, Mar. 2011.

[37] W. Li, C. Liang, W. Zhou, J. Qiu, Z. Zhou, G. Sun, and Q. Xin, "Preparation and characterization of multiwalled carbon nanotube-

supported platinum for cathode catalysts of direct methanol fuel cells," *J. Phys. Chem. B*, vol. 107, no. 26, pp. 6292–6299, 2003.
[38] I. Stamatin, A. Morozan, A. Dumitru, V. Ciupina, G. Prodan, J. Niewolski, and H. Figiel, "The synthesis of multi-walled carbon nanotubes (MWNTs) by catalytic pyrolysis of the phenol-formaldehyde resins," *Phys. E Low-dimensional Syst. Nanostructures*, vol. 37, no. 1, pp. 44–48, 2007.
[39] L. Bokobza and J. Zhang, "Raman spectroscopic characterization of multiwall carbon nanotubes and of composites." *Express Polym. Lett.,* vol. 6, no. 7, 2012.
[40] R. Leyva Ramos, L. A. Bernal Jacome, J. Mendoza Barron, L. Fuentes Rubio, and R. M. Guerrero Coronado, "Adsorption of zinc (II) from an aqueous solution onto activated carbon," *J. Hazard. Mater.,* vol. 90, no. 1, pp. 27–38, 2002.
[41] D. Mohan, V. K. Gupta, S. K. Srivastava, and S. Chander, "Kinetics of mercury adsorption from wastewater using activated carbon derived from fertilizer waste," *Colloids Surfaces A Physicochem. Eng. Asp.,* vol. 177, no. 2, pp. 169–181, 2000.
[42] M. Zabihi, A. Ahmadpour, and A. H. Asl, "Removal of mercury from water by carbonaceous sorbents derived from walnut shell," *J. Hazard. Mater.,* vol. 167, no. 1, pp. 230–236, 2009.
[43] C. Jeon and K. Ha Park, "Adsorption and desorption characteristics of mercury (II) ions using aminated chitosan bead," *Water Res.,* vol. 39, no. 16, pp. 3938–3944, 2005.
[44] D. Tiwari, "Biomass-derived materials in the remediation of heavy-metal contaminated water: Removal of cadmium (II) and copper (II) from aqueous solutions," *Water Environ. Res.,* vol. 83, no. 9, pp. 874–881, 2011.
[45] F. J. Cerino-Córdova, A. M. García-León, E. Soto-Regalado, M. N. Sánchez-González, T. Lozano-Ramírez, B. C. García-Avalos, and J. A. Loredo-Medrano, "Experimental design for the optimization of copper biosorption from aqueous solution by Aspergillus-terreus," *J. Environ. Manage.,*vol. 95, pp. S77–S82, 2012.
[46] N. Li and R. Bai, "Copper adsorption on chitosan–cellulose hydrogel beads: behaviors and mechanisms," *Sep. Purif. Technol.,* vol. 42, no. 3, pp. 237–247, 2005.
[47] I. Langmuir, "The adsorption of gases on plane surfaces of glass, mica and platinum.," *J. Am. Chem. Soc.,* vol. 40, no. 9, pp. 1361–1403, 1918.
[48] F. H. Uber, "Die adsorption in losungen," *Z. Phys. Chem,* vol. 57, pp. 387–470, 1985.
[49] M. I. Temkin and V. Pyzhev, "Kinetics of ammonia synthesis on promoted iron catalysts," *Actaphysiochim.* URSS, vol. 12, no. 3, pp. 217–222, 1940.
[50] M. M. Dubinin, E. D. Zaverina, and L. V Radushkevich, "Sorption and structure of active carbons. I. Adsorption of organic vapors," *ZhurnalFiz. Khimii,* vol. 21, pp. 1351–1362, 1947.